

# Magneto-transport properties of monolayer borophene in perpendicular magnetic field: influence of electron-phonon interaction

Ta T. Tho<sup>1</sup>, Huynh T. Hoa<sup>2</sup>, Nguyen V. Chuong<sup>3</sup>, Luong M. Tuan<sup>1</sup>, Bui D. Hoi<sup>2,4,\*</sup>

<sup>1</sup>Department of Physics, Faculty of Mechanical Engineering, National University of Civil Engineering, 55 Giai Phong St., Hai Ba Trung Dist., Hanoi, Viet Nam

<sup>2</sup>Department of Physics, University of Education, Hue University, 34 Le Loi St., Hue, Viet Nam

<sup>3</sup>Department of Materials Science and Engineering, Le Quy Don Technical University, 236 Hoang Quoc Viet St., Nam Tu Liem Dist., Hanoi, Viet Nam

<sup>4</sup>Center for Theoretical and Computational Physics, University of Education, Hue University, 34 Le Loi St., Hue, Viet Nam

\* Correspondence to Bui D. Hoi <buidinhhoi@hueuni.edu.vn>

(Received: 27 October 2021; Accepted: 17 November 2021)

**Abstract.** The magneto-transport properties of a borophene monolayer in a perpendicular magnetic field  $B$  are studied via calculating the conductivity tensor and resistance under electron-optical phonon interaction by using the linear response theory. Numerical results are obtained and discussed for some specific parameters. The magnetic field-dependent longitudinal conductivity shows the magneto-phonon resonance effect that describes the transition of electrons between Landau levels by absorbing/emitting an optical phonon. The Hall conductivity increases first and then decreases with the magnetic field strength. Also, the longitudinal resistance increases significantly with increasing temperature, which shows the metal behaviour of the material. Practically, the observed magneto-phonon resonance can be applied to experimentally determine some material parameters, such as the distance between Landau levels and the optical phonon energy.

**Keywords:** borophene, magneto-transport, conductivity, resistance, electron-phonon interaction

## 1 Introduction

Since the discovery of graphene, other two-dimensional (2D) materials, such as graphene, hexagonal boron nitride, silicene, germanene, phosphorene, transition metal dichalcogenides, and arsenene, have drawn dramatically increasing attention in recent years owing to their unique electronic, superconductive, elastic, thermal, anisotropic mechanical, optical, and transport properties. Recently, there has been intense research interest in 2D crystalline boron structures, referred to as borophene, because of its anisotropic tilted Dirac cone after its experimental realization. Since boron locates between

nonmetallic carbon and metallic beryllium in the periodic table, there are merely three valence electrons in boron  $[\text{He}] 2s^2 2p^1$ . The  $2p$  electron and its orbit radius are close to that of the  $2s$  state, endowing it with both metallicity and non-metallicity. Such a unique electronic structure of boron enables the formation of highly diverse bondings, ranging from strongly covalent two-centre bonds to metallic-like multi-centre bonds [1]. From the first-principles calculations, the electronic properties of borophene are studied and proved that the Dirac cones are actually formed by the  $p_z$  orbitals of the inequivalent sublattices [2]. The low-energy effective

Hamiltonian of borophene [3, 4], the density response function [5], the optical conductivity [6], the nonlinear Hall effect [7], and the electronic dynamics under the action of surface optical phonons [8] have been reported. Unlike graphene, borophene possesses a powerful anisotropic structure, and its electronic and magnetic properties can be directionally controlled to achieve flexible optical applications [9].

On the other hand, when a uniform magnetic field is applied perpendicularly to the plane of a two-dimensional electron system, the energy spectrum of carriers is quantized into Landau levels. This quantization leads to some novel effects in the system, such as the Hall effect, magneto-phonon resonance effect, and Shubnikov-de Haas oscillations. The magneto-transport of monolayer borophene is also expected to exhibit interesting behaviours. Therefore, in this work, we investigate the magneto-transport properties of monolayer borophene subjected to a perpendicular magnetic field, considering the electron-optical phonon scattering effect. The rest of the paper is organized as follows. In Sec. 2, we briefly present the theoretical model and analytical results for the conductivity tensor and resistance. Section 3 shows numerical results and discussion. Finally, the results are summarised briefly in Sec. 4.

## 2 Theoretical model and analytical results

We consider a two-dimensional borophene sheet where charged carriers move freely in the  $(x, y)$  plane. When a uniform static magnetic field  $\vec{B}$  is applied perpendicularly to the borophene sheet, namely in the  $z$ -direction, the low-energy Hamiltonian, established by using the Peierls substitution  $\vec{p} \rightarrow \vec{p} + e\vec{A}$  with the vector potential  $\vec{A} = (0, xB, 0)$ , is given as

$$H = \xi \left[ v_{0x} p_x \sigma_x + v_{0y} (p_y + eBx) \sigma_y \right] \quad (1)$$

where  $\xi = +1(-1)$  for the  $K(K')$  valley;  $e$  is the electron charge;  $(v_{0x}, v_{0y}) = (0.86v_0, 0.69v_0)$  ( $v_0 = 10^6 \text{ m}\cdot\text{s}^{-1}$ ) are the velocity components in the  $x$  and  $y$ -direction.

Also,  $\sigma = (\sigma_x, \sigma_y)$  are the pseudo-Pauli matrices. Note that the velocities along the  $x$  and  $y$ -direction are not identical. The eigenfunction-eigenvalue problem corresponding to Hamiltonian (1) has been reported in detail in [10]. The energy and the wave function of a charged carrier are given by

$$E_\zeta = \lambda \hbar \omega_c \sqrt{2n}, \quad (2)$$

and

$$\psi_\zeta(\vec{r}) \equiv |\zeta\rangle = \frac{e^{ik_y y}}{\sqrt{2L_y}} \begin{pmatrix} \xi \lambda \phi_{n-1}(X) \\ i \phi_n(X) \end{pmatrix}, \quad (3)$$

where  $\lambda = +1(-1)$  corresponds to the conduction (valence) band;  $n$  ( $= 0, 1, 2, \dots$ ) is the Landau energy level index;  $\omega_c$  ( $= v_c / l_c$ ) is the cyclotron frequency with  $v_c = \sqrt{v_{0x} v_{0y}}$  and  $l_c = \sqrt{\hbar / eB}$ ,  $\vec{r} = (x, y)$  is the spatial coordinate in the borophene plane;  $\phi_n(X)$  is the simple harmonic oscillator wave function;  $X = (x + x_0) / l_c$ ,  $x_0 = k_y l_c^2$ ,  $k_y$  and  $L_y$  are the wave number and normalization length in the  $y$ -direction [10].

Within the linear response theory [11-13], we have the general expressions for the longitudinal ( $\sigma_{xx}$ ) and the Hall ( $\sigma_{yx}$ ) conductivity in the borophene sheet as

$$\sigma_{xx} = \frac{\beta e^2}{A} \sum_{\xi, \xi'} f_{\xi} (1 - f_{\xi'}) W_{\xi\xi'} (\chi_{\xi} - \chi_{\xi'})^2, \quad (4)$$

$$\sigma_{yx} = \frac{ie^2 \hbar}{A} \sum_{\xi \neq \xi'} \frac{f_{\xi'} - f_{\xi}}{(E_{\xi'} - E_{\xi})^2} \langle \xi' | v_x | \xi \rangle \langle \xi | v_y | \xi' \rangle, \quad (5)$$

where  $\beta = 1/(k_B T)$  with  $T$  being the sample temperature;  $A$  is the normalization area;  $f_{\xi}$  is the Fermi-Dirac distribution function for electron at state  $|\xi\rangle$ ,  $\chi_{\xi} = \langle \xi | x | \xi \rangle$ ,  $\chi_{\xi'} = \langle \xi' | x | \xi' \rangle$ , and  $W_{\xi\xi'}$  is the transition rate between states  $|\xi\rangle$  and  $|\xi'\rangle$ . In this study, we consider the high temperature range so that the electron-optical phonon interaction is dominant, and other interactions can be neglected. The electron transition rate is then given by

$$W_{\xi\xi'} = \frac{2\pi}{\hbar} g_s g_v \sum_{\vec{q}} |C(\vec{q})|^2 g(\theta) |J_{m'}(u)|^2 \times \left[ N_{\vec{q}} \delta_{k_y, k_y' + q_y} \delta(E_{\xi} - E_{\xi'} + \hbar\omega_{\vec{q}}) + (1 + N_{\vec{q}}) \delta_{k_y, k_y' - q_y} (E_{\xi} - E_{\xi'} - \hbar\omega_{\vec{q}}) \right] \quad (6)$$

where  $g_s = 2$  and  $g_v = 2$  are the valley and spin degeneracy;  $C(\vec{q})$  is the Fourier transformation of the electron-optical phonon interaction potential;  $g(\theta) = \cos^2(\theta/2)$  is the overlap integral of spin or wave function;  $N_{\vec{q}}$  is the distribution function of phonons with energy  $\hbar\omega_{\vec{q}}$  and wave vector  $\vec{q}$ , and

$$|J_{m'}|^2 = \frac{1}{4} \frac{m!}{(m+j)!} e^{-u} u^j \times \left[ L_m^j(u) + \xi \lambda \xi' \lambda' \sqrt{\frac{m+j}{m}} L_{m-1}^j(u) \right]^2 \quad (7)$$

$$|C(\vec{q})|^2 = \frac{\hbar D_{op}^2}{2\rho A \omega_{\vec{q}}}. \quad (8)$$

where  $u = l_c^2 q^2 / 2$ ,  $q = q_x^2 + q_y^2$ ,  $m = \min(n, n')$ ,  $j = |n' - n|$  and  $L_m^j(u)$  is the associated Laguerre polynomial;  $D_{op}$  is the electron-optical phonon interaction constant, and  $\rho$  is the 2D mass density.

From the wave functions (3), one can derive the following matrix elements needed for the calculation of  $\sigma_{xx}$  and  $\sigma_{yx}$

$$\langle \xi | x | \xi \rangle = l_c^2 k_y, \quad (9)$$

$$\langle \xi' | x | \xi' \rangle = l_c^2 k_y', \quad (10)$$

$$\langle \xi' | v_x | \xi \rangle = \frac{i\xi v_c}{2} \left[ \xi' \lambda' \delta_{n-1, n} - \xi \lambda \delta_{n, n-1} \right] \delta_{k_y, k_y'}, \quad (11)$$

$$\langle \xi | v_y | \xi' \rangle = \frac{\xi v_c}{2} \left[ \xi \lambda \delta_{n-1, n} + \xi' \lambda' \delta_{n, n-1} \right] \delta_{k_y, k_y'}. \quad (12)$$

We now adopt the assumption that phonons are dispersionless, i.e.,  $\hbar\omega_{\vec{q}} \approx \hbar\omega_0 =$  constant and  $\langle N_{\vec{q}} \rangle_{eq} \approx N_0 = \left[ \exp(\hbar\omega_0 / k_B T) - 1 \right]^{-1}$ .

Also, we change the summation over  $k_y$  as

$$\sum_{k_y} \rightarrow \frac{L_y}{2\pi} \int_0^{L_x/l_c^2} dk_y \int_0^\pi d\theta = \frac{A}{2l_c^2}.$$

Furthermore, from the delta Kronecker in Eq. (6) one has

$$(k_y' - k_y) = q_y, \text{ and so } (\chi_{\xi} - \chi_{\xi'})^2 = (q_y l_c^2)^2.$$

After some manipulation, we obtain the expressions for  $\sigma_{xx}$  and  $\sigma_{yx}$  as

$$\begin{aligned}
 \sigma_{xx} = & \frac{\beta e^2 D_{op}^2}{8\rho\omega_c^2} \sum_{n,n'} f_n (1-f_{n'}) \\
 & \times \left\{ (2m+j+1) - 2\xi\lambda\xi'\lambda' \sqrt{m(m+j)} \right. \\
 & \left. + (\xi\lambda\xi'\lambda')^2 (2m+j-1) \right\} \left\{ N_0 \delta(E_n - E_{n'} + \hbar\omega_0) \right. \\
 & \left. + (1+N_0) \delta(E_n - E_{n'} - \hbar\omega_0) \right\}, \quad (13)
 \end{aligned}$$

$$\begin{aligned}
 \sigma_{yx} = & \frac{e^2 \xi^2}{8\hbar} \sum_{n,n'} \frac{f_{n'} - f_n}{\left( \lambda' \sqrt{2n'} - \lambda \sqrt{2n} \right)^2} \\
 & \times \left( \xi^2 \lambda^2 \delta_{n-1,n'} - \xi'^2 \lambda'^2 \delta_{n,n'-1} \right), \quad (14)
 \end{aligned}$$

where we have redenoted  $f_\zeta \equiv f_n$  and  $E_\zeta \equiv E_n$ . Following the collision-broadening model for electron-phonon scattering, we replace the delta functions in Eq. (13) with the Lorentzians as

$$\delta(\varepsilon) = \frac{\Gamma}{\pi(\varepsilon^2 + \Gamma^2)}, \quad (15)$$

where  $\Gamma$  is the broadening parameter that depends on the scattering mechanism and has the unit of energy. In this calculation, we take phenomenologically  $\Gamma = 0.02\hbar\omega_c$ .

Finally, the longitudinal resistance is obtained from the conductivity tensor components as [14]

$$\rho_{xx} = \frac{\sigma_{xx}}{\sigma_{xx}^2 + \sigma_{yx}^2}. \quad (16)$$

### 3 Numerical results and discussion

In this section, we numerically evaluate the conductivity tensor and resistance components and clarify their behaviour with changing the

parameters. Figure 1 shows the dependence of the longitudinal conductivity on the magnetic field strength at two values of optical phonon energy. We can see the maxima in the plot of  $\sigma_{xx}$ . We can explain the physical meaning of these maxima as follows. For the case of  $\hbar\omega_0 = 42$  meV (the dashed curve), the peaks from left to right correspond to the magnetic field strength of 2.255, 4.209, 6.573, and 13.146 T, respectively. We can deduce that these peaks satisfy the condition

$$E_{n'} - E_n - \hbar\omega_0 = 0. \quad (17)$$

This condition describes the magneto-phonon resonance in which an electron at the Landau level  $E_n$  transits to the level  $E_{n'}$  by absorbing an optical phonon of energy  $\hbar\omega_0$ . The first, the second, the third, and the fourth peak correspond to the transition  $(n, n') = (1, 4)$ ,  $(1, 3)$ ,  $(2, 4)$ , and  $(1, 2)$ , respectively. From the figure, we can also see that the longitudinal conductivity decreases with increasing magnetic field strength. This is reasonable and agrees with that observed in semiconductors as well as 2D materials in magnetic fields.

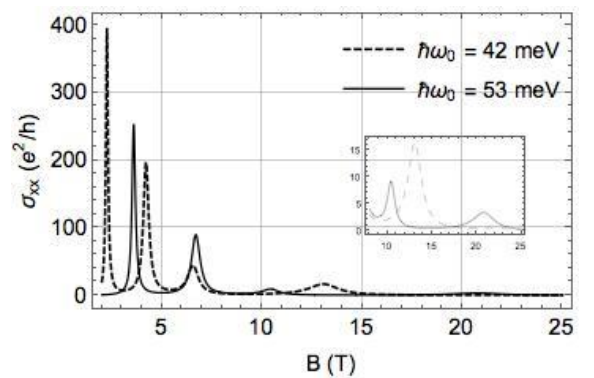


**Fig. 1.** Longitudinal conductivity as a function of magnetic field strength at two values of optical phonon energy:  $\hbar\omega_0 = 53$  meV (solid curve) and  $\hbar\omega_0 = 42$  meV (dashed curve). Here,  $T = 200$  K.

In Fig. 2, the longitudinal resistance is also plotted versus  $B$  at the phonon energy of 42 meV. There is an oscillation of the longitudinal resistance with the magnetic field. The amplitude of the resistance increases with increasing magnetic field strength. Also, the resistance has minimum values when the conductivity is maximum and vice versa, as shown in the figure.

The dependence of the longitudinal resistance on temperature is shown in Fig. 3. It can be seen that the longitudinal resistance increases considerably with increasing

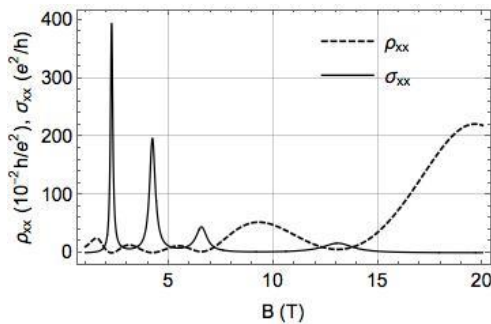


**Fig. 2.** Longitudinal conductivity (solid curve) and longitudinal resistance (dashed curve) versus magnetic field strength at the optical phonon energy of 42 meV. Here,  $T = 200$  K.

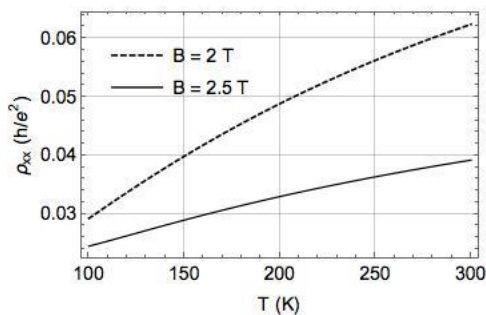


**Fig. 3.** Longitudinal resistance as a function of temperature at  $B = 2.5$  T (solid curve) and  $B = 2$  T (dashed curve). Here,  $\hbar\omega_0 = 42$  meV.

temperature. This increase demonstrates the metallic characteristic and agrees that monolayer borophene is a semimetal where the conduction and the valance bands meet at the Dirac point.

Fig. 4 shows the dependence of the Hall conductivity on the magnetic field strength at different temperatures. We can see that the Hall conductivity increases and then decreases with magnetic field strength. Also, the Hall conductivity seems to reach saturation in the region of very strong magnetic fields.

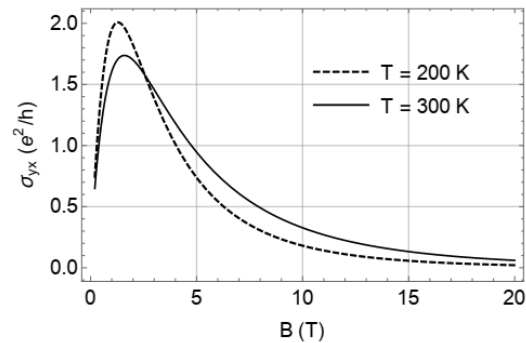


**Fig. 4.** Hall conductivity as a function of magnetic field strength at 300 K (solid curve) and 200 K (dashed curve).

## 4 Conclusion

We studied the magneto-transport properties of monolayer borophene in a perpendicular magnetic field under electron-optical phonon interaction. The conductivity tensor and resistance were calculated by using the linear response theory. We found that the magnetic field-dependent longitudinal conductivity exhibits the magneto-phonon resonance effect that describes the transition of electrons between Landau levels because the material absorbs/emits an optical phonon. The Hall conductivity depends strongly on the magnetic field strength. Furthermore, the longitudinal resistance increases significantly with increasing temperature. The obtained results give an insight into the magneto-electrical transport properties of monolayer borophene in

strong magnetic fields at ambient temperature, which can open possible applications of the material to nano-electronic devices.

### Funding statement

This research was funded by Hanoi University of Civil Engineering (HUCE) under grant number 29-2021/KHXD-TĐ.

### References

1. Fujimori M, Nakata T, Nakayama T, Nishibori E, Kimura K, Takata M, et al. Peculiar Covalent Bonds in  $\alpha$ -Rhombohedral Boron. *Physical Review Letters*. 1999;82(22):4452-4455.
2. Lopez-Bezanilla A, Littlewood PB. Electronic properties of 8-Pmmn borophene. *Physical Review B*. 2016; 93 (24):241405.
3. Nakhaee M, Ketabi SA, Peeters FM. Tight-binding model for borophene and borophane. *Physical Review B*. 2018;97(12):125424.
4. Zabolotskiy AD, Lozovik YE. Strain-induced pseudomagnetic field in the Dirac semimetal borophene. *Physical Review B*. 2016;94(16):165403.
5. Krishanu S, Amit A. Anisotropic plasmons, Friedel oscillations, and screening in 8-Pmmn borophene. *Physical Review B*. 2017;96(3): 035410.
6. Verma S, Mawrie A, Ghosh TK. Effect of electron-hole asymmetry on optical conductivity in 8 Pmmn borophene. *Physical Review B*. 2017;96(15):155418.
7. Jing L, Tian X, Guo-Bao Zhu, Hui P. Photoinduced anomalous Hall and nonlinear Hall effect in borophene. *Solid State Communications*. 2020;322: 114092.
8. Akay D. Manipulating electronic dynamics of 8-Pmmn borophene with surface optical phonons. *Semiconductor Science and Technology*. 2021;36(4): 045001.
9. Zhongjian X, Xiangying M, Xiangnan L, Weiyuan L, Weichun H, Keqiang C, et al. Two-Dimensional Borophene: Properties, Fabrication, and Promising Applications. *Research*. 2020;2020:2624617.
10. Islam SF. Magnetotransport properties of 8-Pmmn borophene: effects of Hall field and strain. *Journal of Physics: Condensed Matter*. 2018;30(27):275301.
11. Charbonneau M, van Vliet KM, Vasilopoulos P. Linear response theory revisited III: One-body response formulas and generalized Boltzmann equations. *Journal of Mathematical Physics*. 1982; 23(2):318-336.
12. Vasilopoulos P. Magnetophonon oscillations in quasi-two-dimensional quantum wells. *Physical Review B*. 1986; 33(12):8587.
13. Vasilopoulos P, Charbonneau M, van Vliet KM. Linear and nonlinear electrical conduction in quasi-twodimensional quantum wells. *Physical Review B*. 1987;35(3):1334.
14. Castro Neto AH, Guinea F, Peres NMR, Novoselov KS, Geim AK. The electronic properties of graphene. *Reviews of Modern Physics*. 2009; 81(1):109-162.